



>> Monitoring cancer spheroid growth and cytotoxicity with Omni live-cell imager

Key findings:

- Effects of doxorubicin on C6 spheroids can be evaluated with brightfield and fluorescence imaging using the Omni platform
- C6 spheroid formation occurs in a two-phase process, aggregation, and growth
- Doxorubicin has a dose-dependent effect on C6 spheroids

Introduction

Cancer accounts for a significant number of deaths worldwide and continues to be the second leading cause of mortality¹. The invasiveness of the type of cancer plays a major role in determining treatment options and survival. Highly invasive, difficult-to-treat cancer types include glioblastoma and other high-grade malignant brain tumors, non-small cell lung cancer, and triple-negative breast cancer². These tumors are characterized by genetic mutations in oncogenes and tumor suppressor genes. In combination with their highly invasive nature, these mutations pose significant challenges for effective treatment³⁻⁵.

Traditionally, two-dimensional (2D) monolayer cell cultures have been used to investigate the antitumor activity of a therapeutic compound. Those culture methods are relatively straightforward, cost-effective, and ideal for high-

Abstract

Three-dimensional (3D) cell cultures such as spheroids and organoids serve as a representative model for tumors and the interaction with the microenvironment. Here, the Omni live-cell imaging platform was used to monitor and analyze spheroid formation for multiple cell types. Additionally, the uptake and effect of the chemotherapy drug doxorubicin on spheroids were monitored on the Omni, demonstrating its use as a valuable tool for evaluating drug impact on 3D models.

throughput screening using well-established assays. However, monolayer cultures present a simplified version of tumors that may insufficiently capture essential cellular organization and interactions found in vivo^{6,7}. To overcome these limitations, three-dimensional (3D) cell culture models such as spheroids and organoids are increasingly developed in research. 3D cultures have emerged as powerful tools in tumor research, primarily due to their ability to better mimic the natural microenvironment^{8,9}. Spheroids, which are self-assembled cell aggregates, exhibit more complex cell-cell interactions as well as a nutrient and oxygen gradient, making them promising models for drug treatment and drug development studies, especially in oncology research^{10,11}.

Despite their advantages over 2D cultures, 3D models also have limitations, including higher cost



and variability in spheroid formation efficiency. These challenges highlight the necessity to optimize culture methods. Additionally, assays traditionally designed for 2D setups may pose challenges when adapted to suit the complexities of 3D cultures^{12,13}. Live-cell imaging presents a valuable tool in oncology research using spheroids, as it enables continuous monitoring of spheroid development in size and morphology. This method will facilitate evaluation of various culture methods and supports drug treatment analysis by providing kinetic data on drug uptake and cytotoxicity.

In this study, the Omni live-cell imaging platform was used to monitor the effect of doxorubicin (DOX) on cancer spheroids to demonstrate the benefits of live-cell imaging in analyzing drug studies with 3D cell culture models. First, formation and growth of various cancer spheroids was characterized. C6 cells (rat glial cells), A549 cells (adenocarcinomic human alveolar basal epithelial cells), and MDA-MB-231 cells (human epithelial mammary adenocarcinoma cells) were used as they serve as a valuable model for glioblastoma, lung cancer, and triple negative breast cancer, respectively¹⁴⁻¹⁶. DOX, an anthracycline drug, is widely used as an antitumor agent in the treatment of various types of cancer, including breast, lung, ovarian, and brain tumors¹⁷. Therefore, after the characterization of spheroid formation, C6 spheroids were exposed to various concentrations of DOX to assess its effect on their growth.

Materials and Methods

Cells and reagents

C6 cells (ATCC, Cat. CCL-107) were maintained in DMEM medium (Gibco, Cat. 41965039) supplemented with 10% fetal bovine serum (FBS; Gibco, Cat. 16000044) and 1%

penicillin/streptomycin (Gibco, Cat. 15140122). A549 cells (Innoprot, Cat. P20118) were maintained in Ham's F-12K medium (Gibco, Cat. 21127022) supplemented with 10% FBS (Gibco, Cat. 16000044) and 250 µg/mL G418 (Gibco, Cat. 10131035). MDA-MB-231 cells (Innoprot, Cat. P20317) were maintained in RPMI medium (Gibco, Cat. 11875093), 10% FBS (Gibco, Cat. 16000044), 1% penicillin/streptomycin (Gibco, Cat. 15140122) and 10 µg/mL puromycin dihydrochloride (Gibco, Cat. A1113803). Cells were passaged every 3 days when confluence reached 80%.

Cancer spheroid formation

First, a 96-well U-bottom plate (VWR, Cat. 734-2782) was prepared by adding 100 µL Anti-Adherence Rinsing Solution (STEMCELL Technologies, Cat. 07010) to each well that was used. The plate was incubated for 5 minutes at room temperature, followed by aspiration of the Anti-Adherence Rinsing Solution. The wells were washed by adding 100 µL PBS, incubating for 5 minutes, and aspirating the PBS.

C6 cells, A549 cells, and MDA-MB-231 cells were lifted from flasks and dissociated via trypsinization and subsequently counted using the Exact FL. Next, the cells were centrifuged and resuspended in appropriate medium to the desired working concentrations. Cells were introduced to the pre-treated U-bottom plate by adding 100 µL of cell suspension per well, resulting in the respective final cell densities of 1,000, 1,250, 2,500, 5,000, and 10,000 cells per well. The plate was centrifuged at 1000 rpm for 4 minutes. The well plate was placed on the Omni inside an incubator at 37 °C and 5% CO₂. Spheroid formation was monitored simultaneously across all cell types over 72 hours using the Omni platform with a time interval of 3 hours. During brightfield acquisition, the camera scans the



sample stage while acquiring a series of sequential images that are stitched together to create a total surface area image. This allows for the assessment of all spheroids simultaneously. Data analysis was performed using the Axion Portal.

Doxorubicin dose-response assay

C6 spheroids were prepared as described before using a final cell density of 2,500 cells per well. DOX (Sigma, CAS-no: 25316-40-9) was diluted to 2x the desired final concentration from the stock solution using the appropriate cell culture medium. After 72 hours of spheroid formation, 100 μL of DOX solution was added to each well containing the spheroid in 100 μL of medium, yielding final concentrations of 0, 5, 10, 20 and 32 μM . The well plate was placed on the Omni inside an incubator at 37 $^{\circ}\text{C}$ and 5% CO_2 . DOX uptake was monitored over 72 hours by imaging every hour.

As DOX is inherently red fluorescent, an increase in red fluorescence indicates DOX uptake. The size of the spheroid and the red fluorescence object intensity within spheroids were analyzed using the Axion Portal. As the size of the spheroid influences the fluorescence intensity, the object intensity was normalized using the following equation:

$$\text{Normalized object intensity} = \frac{I(t)}{A(t)}$$

where $I(t)$ represents the intensity at time t and $A(t)$ represents the area at time t .

Results

Real-time monitoring of cancer spheroid formation and growth

To investigate the effect of DOX on cancer spheroids, the optimal seeding density and spheroid culture time had to be determined first.

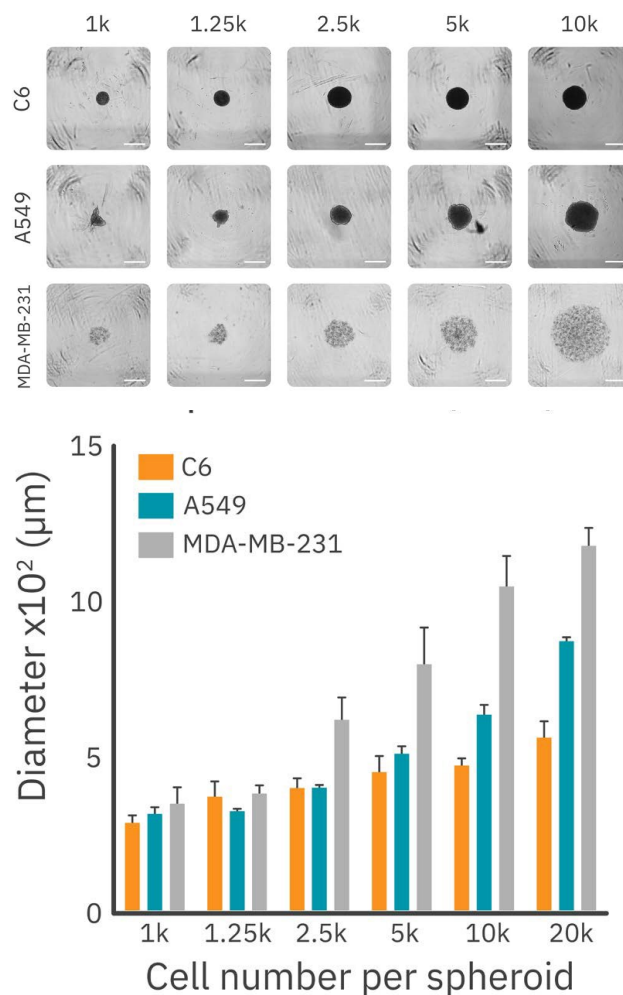
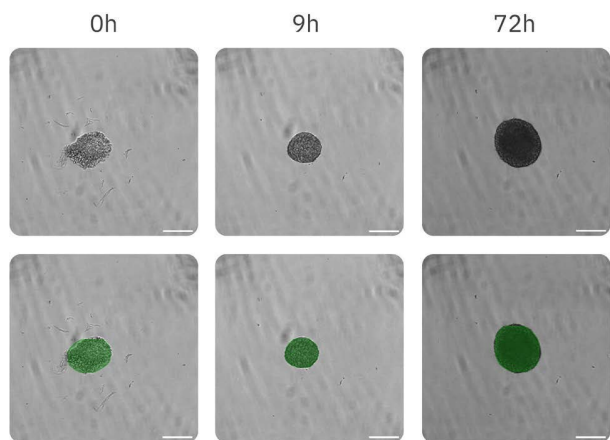


Figure 1: (Top) Images of spheroids from C6, A549, and MDA-MB-231 cells (top to bottom) using cell densities between 1,000 and 10,000 cells per well (left to right). The scale bar represents 200 μm . (Bottom) Quantitative assessment of spheroid size for the varying conditions 72 hours after seeding ($n=3$). The error bars represent standard deviation.

Various seeding densities were investigated for a 72-hours period (**Fig. 1**). The brightfield images (**Fig. 1, top**) showed that the different cell types form varying types of spheroids. C6 and A549 cells both form compact spheroids, whereas MDA-MB-231 form loose clusters of cells instead of a compact spheroid. The A549 spheroids are more irregularly shaped compared to the C6 spheroids. As C6 cells form the most round and compact spheroids, C6 cells were used for the remaining experiments.



C6 spheroid size

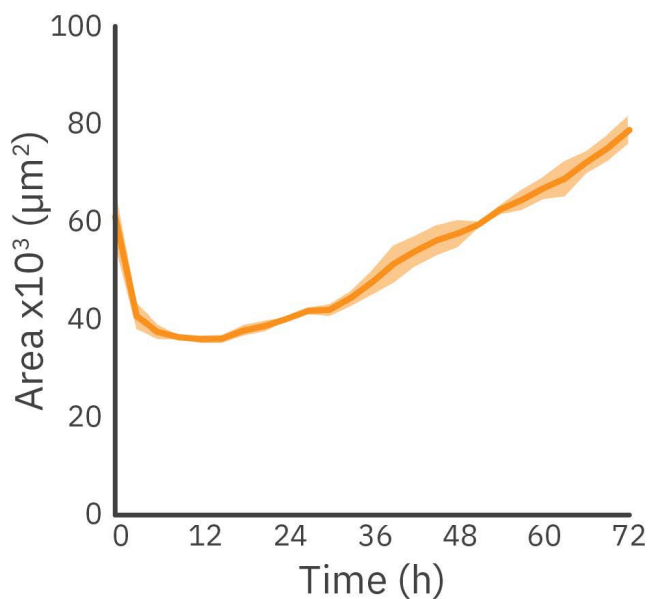


Figure 2: (Top) Images acquired by the Omni of C6 spheroids cultured over time. The bottom images show the Organoid Analysis module overlay. The scale bar represents 200 μm. (Bottom) Quantitative assessment of spheroid size over time (n=3). The error bars represent standard deviation.

Figure 1 displays the size of the different types of spheroids for the varying seeding densities. According to existing literature, spheroids exceeding 500 μm in diameter tend to develop necrotic regions¹⁸. To address this, 2,500 cells per well was chosen as the optimal seeding density. This condition ensures the formation of stable midsized spheroids without necrotic regions and facilitates ongoing growth for the duration of the

drug treatment experiments. This seeding density was used to further characterize the growth pattern of C6 spheroids.

As shown in **Figure 2**, the formation and growth behavior of C6 spheroids at a seeding density of 2,500 cells per well can be divided into two phases: the formation phase and the growth phase. During the first phase, dispersed cells aggregate to form the spheroid, resulting in an initial decrease in size. The duration of this phase can vary based on cell type and seeding density. For C6 cells with a seeding density of 2,500 cells per well, it takes approximately 9 hours. Following this initial phase, the second phase commenced, during which the spheroids expand.

Doxorubicin inhibits spheroid growth

The effect of increasing concentrations of DOX on C6 spheroids is shown in **Figure 3**. The fluorescence images (**Fig. 3**) demonstrate the progressive uptake of DOX by the spheroids over time.

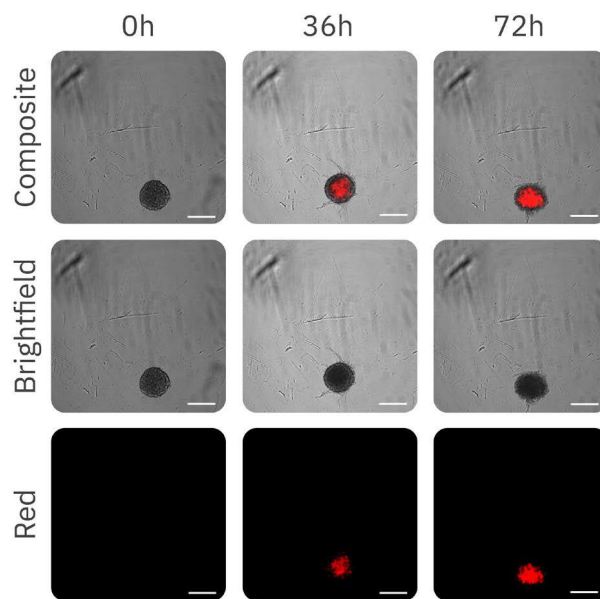


Figure 3: Brightfield, red fluorescence, and composite images of the spheroid over time exposed to 5 μM of doxorubicin. The scale bar represents 200 μm.



For more insight into the effect of DOX uptake, the object intensity was used to analyze the intensity increase over time (Fig. 4). The expected uptake is confirmed by the analysis of the fluorescence intensity within the spheroid over time. As shown in Figure 4, there was a fast uptake of DOX. Notably, higher concentrations result in a more substantial internalization by the spheroid. Additionally, the uptake pattern significantly varies among the lowest and highest concentrations. Lower concentrations (5 and 10 μM) display a similar and stable increase in intensity until it reaches a maximum after approximately 42 hours. This is followed by a decrease in fluorescence intensity. The uptake pattern of the higher concentrations (20 and 32 μM) is characterized by a fast uptake indicated by the increase in intensity, followed by a weaker and slower increase in fluorescence intensity indicating continuation of the uptake of DOX. This data suggests higher concentrations of DOX have a different effect on spheroids. However, more extensive research is required to confirm this.

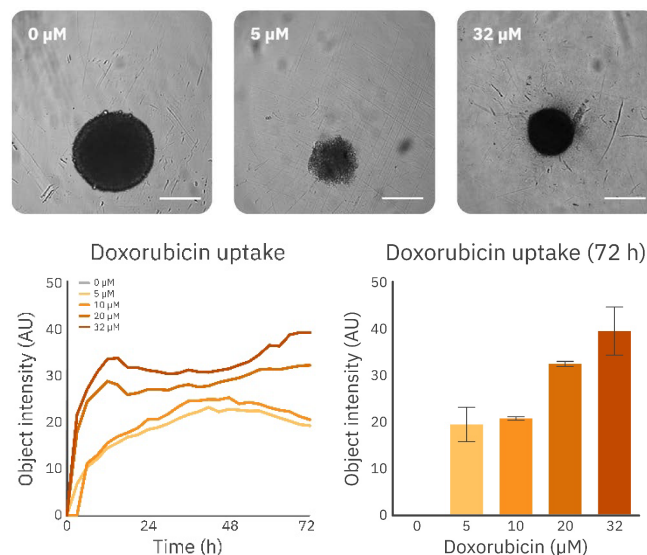


Figure 4: (Bottom, left) Normalized fluorescence object intensity of the DOX uptake by the spheroid over 72 hours for concentrations of 0, 5, 10, 20, and 32 μM ($n=2$). (Bottom, right) Normalized object intensity at 72 hours ($n=2$) with significant differences observed between all groups except for 5 μM compared to 10 μM and 20 μM compared to 32 μM ($p<0.001$). The error bars represent standard deviation.

Conclusion

This study demonstrates the advantages of using the Omni live-cell imaging platform to track cancer spheroid formation and assess the effect of antitumor compounds on complex 3D cell culture models. We demonstrated a simple, automated approach that can support evaluation of spheroid culture by tracking spheroid size. Furthermore, the Omni allowed for efficient drug response assessment in both brightfield and fluorescence.

References

1. Fujii et al. Cause of death among long-term cancer survivors: the NANDE study. *Healthcare* 11(6), March 13, (2023).
2. Siegel et al. Cancer Statistics, 2021. *CA: A Cancer Journal for Clinician* 71, 7-33, (2021).
3. Habashy et al. Challenges in glioblastoma immunotherapy: mechanisms of resistance and therapeutic approaches to overcome them. *British Journal of Cancer* 127, 976-987, (2022).
4. Mogi, A. & Kuwano, H. TP53 mutations in nonsmall cell lung cancer. *Journal of Biomedicine and Biotechnology*, (2021).
5. Ghosh et al. Triple negative breast cancer and non-small cell lung cancer: Clinical challenges and nano-formulation approaches. *Journal of Controlled Release* 337, 27-58, September 10, (2021).
6. Kapalczyńska, M. et al. 2D and 3D cell cultures – a comparison of different types of cancer cell cultures. *Archives of Medical Science* 14(4), 910-919, June (2018).



7. Antoni, D. et al. *Three-dimensional cell culture: a breakthrough in vivo*. *International Journal of Molecular Sciences* 16(3), 5517-5527, March (2015).
8. Gunti et al. *Organoid and Spheroid Tumor Models: Techniques and Applications*. *Cancers* 13(4), 874, Februari (2021).
9. Cacciamali, A., Villa, R. & Dotti, S. *3D Cell cultures: evolution of an ancient tool for new applications*. *Frontiers in Physiology* 13, July (2022).
10. Perche, F. & Torchilin, V. *Cancer cell spheroids as a model to evaluate chemotherapy protocols*. *Cancer Biology & Therapy* 13(12), 1205-1213, October (2012).
11. Thoma et al. *3D cell culture systems modeling tumor growth determinants in cancer target discovery*. *Advanced Drug Delivery Reviews* 69-70, 29-41, April (2014).
12. Huang et al. *Research progress, challenges, and breakthroughs of organoids as disease models*. *Frontiers in Cell and Developmental Biology* 9, November (2021).
13. Hofer, M. & Lutolf, M. *Engineering organoids*. *Nature Reviews Materials* 6, 402-420, (2021).
14. Halas-Wisniewska et al. *The effect of low doses of doxorubicin on the rat glioma C6 cells in the context of the proteins involved in intercellular interaction*. *Acta Histochemica* 122, (2020).
15. Townsend et al. *Non-small-cell lung cancer cell lines A549 and NCI-H460 express hypoxanthine guanine phosphoribosyltransferase on the plasma membrane*. *Onco Targets and Therapy* 10, 1921-1932, (2017).
16. Simu et al. *Insights into the behavior of triple-negative MDA-MB-231 breast carcinoma cells following the treatment with 17 β -ethinylestradiol and levonorgestrel*. *Molecules* 26(9), May, (2021).
17. Zhao, N., Woodle, M. & Mixson, A. *Advances in delivery systems for doxorubicin*. *Journal of Nanomedicine & Nanotechnology* 9(5), (2018).
18. Barisam et al. *Prediction of necrotic core and hypoxic zone of multicellular spheroids in a microbio reactor with a U-shaped barrier*. *Micromachines* 9(3), March, (2018).

Authors

Nathalie Opdam – van de Laar, Application Scientist II

Inge Thijssen – van Loosdregt, Staff Application Scientist

Axion BioSystems, Eindhoven, The Netherlands

Find out more at:

axionbiosystems.com/omni

Or contact us:

axionbiosystems.com/contact

